Low-Cycle Fatigue of Niobium and Niobium-1 Pct Zirconium Alloys

J.M. MEININGER and J.C. GIBELING

Commercially pure niobium (CPNb) and a niobium-1 pct zirconium (Nb-1Zr) alloy were tested under low-cycle fatigue conditions at plastic strain amplitudes in the range of 0.02 pct $\leq \Delta\varepsilon_{pl}/2 \leq 0.7$ pct. At low temperatures, the cyclic deformation response of body-centered cubic (bcc) metals is strongly dependent on strain rate. Thus, it was necessary to test at slow (2×10^{-4} s^{-1}) and fast (2×10^{-2} s^{-1}) strain rates in order to fully characterize the cyclic deformation at ambient temperature. Only cyclic hardening was observed for both metals under all testing conditions. As expected, higher cyclic stresses were recorded at the fast strain rate compared to the slow strain rate. The Nb-1Zr alloy was always stronger than CPNb, although both metals had the same cyclic life at equal plastic strain amplitudes. Further, the strain rate had no effect on the cyclic life. At the fast strain rate, intergranular cracking occurred, and a microplastic plateau was observed in the cyclic stress-strain (CSS) curve for CPNb. At the slow strain rate, no definitely intergranular cracks were detected, and a microplastic plateau was not observed for CPNb. The results of these experiments are interpreted in terms of the influence of strain rate and solute content on the relative mobilities of edge and screw dislocations.

I. INTRODUCTION

IN recent years, there has been an increased interest in obtaining improved elevated-temperature structural materials. Potential applications include the national aerospace plane and space nuclear power systems. Systems such as these will involve cyclic loading imposed by large thermally induced strains. As a consequence, the low-cycle fatigue behavior will be a critical material property in these designs.

Niobium is an attractive candidate for these very high-temperature aerospace applications because it has the lowest density of the refractory metals and has good elevated-temperature strength. Several investigations have been made of the mechanisms of cyclic deformation of single crystals of niobium.[1,2,3] However, very little is known regarding the fatigue behavior of polycrystalline niobium.[4] Chung and Stoloff[5] tested pure polycrystalline niobium under total strain control at a constant frequency. To investigate the fatigue mechanisms, however, it is necessary to use plastic strain as the controlled variable.[6]

Basic research on cyclic deformation of face-centered cubic (fcc) crystals, primarily copper, has resulted in fairly complete understanding of the fatigue mechanisms. In contrast, relatively little fundamental research has been reported for body-centered cubic (bcc) metals, and a detailed, mechanistic understanding is still lacking. However, it has been shown that the cyclic deformation of bcc metals is sensitive to temperature, strain rate, and direction of deformation.[1,2,6]

At low temperatures ($T < 0.2T_m$) or high strain rates at $T \approx 0.2T_m$, bcc metals exhibit a deformation response that is strongly dependent on temperature or strain rate, $\dot{\varepsilon}$. The dependence of the flow stress on temperature and strain rate is usually expressed in terms of an athermal stress and an effective stress as follows:[1,6]

$$\sigma = \sigma_G + \sigma^*(\dot{\varepsilon}, T) \quad [1]$$

where σ_G is the athermal component that arises from the long-range interaction of gliding dislocations with the structure and varies weakly with temperature to the same degree as the shear modulus, and σ^* is the effective stress that depends on $\dot{\varepsilon}$ and T but only weakly on the density and arrangement of the dislocations.

In commercially pure niobium, as with other bcc metals, the physical source of the large effective stress is the limited mobility of the screw dislocations at low temperatures. The glide of the screw dislocations occurs by thermally activated formation of kink pairs. As a result, the mobility of the screw dislocations decreases strongly when the temperature decreases below a critical temperature. For niobium, this critical temperature is close to room temperature for slow strain rates but is higher than room temperature for fast strain rates.[1] In the low-temperature regime, the edge dislocations are more mobile than the screw dislocations, and dislocation multiplication by bowing is difficult. Above the critical temperature, both screw and nonscrew segments have similar mobilities, σ^* is small, and the deformation behavior resembles that of fcc metals.

Besides this stress dependence, the cyclic response of bcc metals is different from that of fcc metals. In single crystals, slip plane and stress asymmetries in tension and compression are observed.[6,7] In cyclic testing, these asymmetries lead to shape changes in the crystals. The slip plane and stress asymmetries are attributed to the extended core structure of the screw dislocations in bcc metals. The effect of the extended core structure is to cause the screw dislocation motion to be dependent not only on the shear stresses in the slip plane but also on the nonshear components; hence, the tension/compression asymmetry.[8]

J.M. MEININGER, Materials Engineer, is with the Science and Engineering Laboratory, McClellan Air Force Base, Sacramento, CA 95652. J.C. GIBELING, Associate Professor, is with the Department of Mechanical, Aeronautical and Materials Engineering, University of California–Davis, Davis, CA 95616.

Manuscript submitted February 24, 1992.

The few available studies of bcc single crystals provide useful information regarding the mechanisms of cyclic deformation. However, no corresponding fundamental studies of polycrystalline metals have been reported. Therefore, the purpose of this investigation was to study the low-cycle fatigue mechanisms in polycrystalline niobium. For comparison, the solid solution-hardened niobium-1 pct zirconium (Nb-1Zr) alloy was tested in addition to the commercially pure niobium (CPNb). In particular, our goal was to identify the effects of strain rate (or temperature) on the cyclic response and to compare the polycrystalline data to the single-crystal results available in the literature.

In order to fully characterize the cyclic deformation behavior of niobium, it was necessary to conduct tests under two separate conditions: (1) where the effective stress was negligible and (2) where the effective stress was a significant fraction of the total stress. Rather than changing the temperature from ambient, the plastic strain rate was varied. The fast (2×10^{-2} s^{-1}) and slow (2×10^{-4} s^{-1}) plastic strain rates were chosen, based on the single-crystal data of Ackermann *et al.*,[1] such that the effective stress would be significant at the fast strain rate but negligible at the slow strain rate. In this way, it was possible to examine the complete range of dislocation behavior in the cyclic deformation of niobium.

II. EXPERIMENTAL PROCEDURE

A. *Description of Materials*

The commercially pure niobium and the niobium-1 pct zirconium alloys were received from Teledyne Wah Chang Albany in annealed 15.9-mm-diameter rod form. The alloys were processed by compacting powder, electron-beam melting, arc remelting, forging, extruding, and hot swaging. They were then annealed at 1473 K for 1 hour at Teledyne Wah Chang Albany to relieve the strain from working. We note that this temperature is not high enough to ensure complete recrystallization.[4] The chemical analyses of the two metals are listed in Table I.

Table I. Chemical Analysis of Metals: Ingot Analysis (Composition in Parts Per Million)

Element	CPNb	Nb-1Zr
Al	< 20	< 20
B	—	< 1
C	< 30	48
Cr	< 20	< 20
Cu	< 40	< 40
Fe	< 50	< 50
H	< 5	< 5
Hf	< 50	< 50
Mo	< 50	< 50
N	23	42
Ni	< 20	< 20
O	< 50	< 50
P	< 25	—
Si	< 50	< 50
Sn	< 10	< 10
Ta	2013	1422
Ti	< 50	< 50
V	< 20	< 20
W	80	78
Zr	< 100	9200

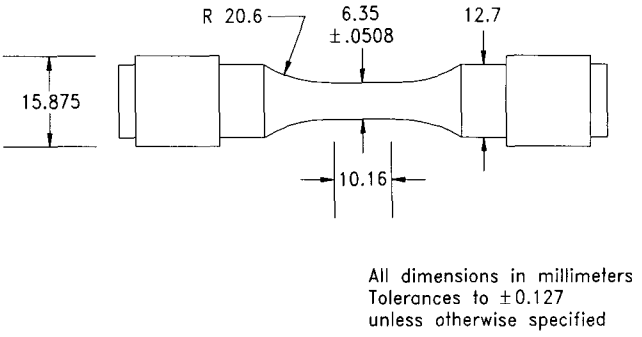

Fig. 1—Low-cycle fatigue specimen dimensions.

B. *Specimen Description and Preparation*

The specimens had a diameter of 6.35 mm and a uniform gage length of 10.2 mm; Figure 1 shows the specimen shape and dimensions. The specimens were machined with the gage length having a maximum 0.81 μm rms finish. After machining, the specimens were successively ground and polished on a lathe using 600 grit sandpaper, then 6- and 1-μm diamond paste. The specimens were tested without further heat treatment.

C. *Low-Cycle Fatigue Test Description*

The cyclic deformation tests were conducted using a fully automated, closed-loop servohydraulic materials test system. The strain was measured with a 7.6-mm gage length extensometer attached to the specimen with rubber bands. Initially, 90-deg extensometer knife edges, with a 0.05-mm edge radius of curvature, were used. However, the knife edges created fairly deep impressions in the soft CPNb material, resulting in crack initiation at the indentations. To minimize this problem, 180-deg blunt knife edges (flat contact edge, 180-deg included angle) were used for all subsequent tests. The specimens were held by mechanical grips of a split collet design. The axis of the specimen was aligned to within ±0.013 mm of the actuator axis during installation.

Typically, a low-cycle fatigue specimen is fully reverse loaded such that the magnitude of the negative strain equals the magnitude of the positive strain. The controlled variable is usually the total strain amplitude. However, since the material response is determined by the plastic strain, the present experiments were conducted using plastic strain amplitude as the controlled variable. The test command signal was saw-toothed (or triangular) in shape. For each individual test, the machine was programmed to maintain a constant total strain rate. However, as outlined below, to achieve a constant average plastic strain rate (at either the fast or slow strain rate), the total strain rate varied with the plastic strain amplitude of the test.

All tests were conducted at room temperature. Both metals were tested at both slow and fast plastic strain rates of 2×10^{-4} s^{-1} and 2×10^{-2} s^{-1}. For a given strain rate (slow or fast), the average plastic strain rate

was maintained constant. This rate is defined by the following equation:[6]

$$\dot{\varepsilon}_{pl} = 2\nu\Delta\varepsilon_{pl} \quad [2]$$

where $\dot{\varepsilon}_{pl}$ is the average plastic strain rate, ν is the frequency, and $\Delta\varepsilon_{pl}$ is the plastic strain range. Given a plastic strain rate and a plastic strain amplitude, the appropriate test frequency was calculated using Eq. [2]. The total strain rate used in the test machine program was determined from the frequency, the plastic strain amplitude, and the elastic strain amplitude estimated from the monotonic data.

Load and strain outputs from the testing machine were converted to digital data pairs by simultaneously triggering two HEWLETT-PACKARD* 3457 digital multimeters. The data pairs were sent to a personal computer for storage and calculation of the outer (plastic strain) loop control parameters. Data were stored in sets of 200 or 400 data pairs that defined individual hysteresis loops.

*HEWLETT-PACKARD is a trademark of Hewlett-Packard Company, Colorado Springs, CO.

At the slow strain rate, real-time computer control was possible. As each load and total strain data pair was obtained, the plastic strain was calculated from these two values; if the desired amplitude had been reached or exceeded, a control signal reversed the loading direction. At the fast strain rate, this mode of real-time control was not possible. Instead, the programmable function generator was used to control the total strain amplitude. Sets of 200 load-strain data pairs corresponding to one or two complete hysteresis loops were acquired and analyzed by the control software to determine the actual plastic strain amplitude. A corrected total strain amplitude setting was then sent to the function generator in order to achieve the desired plastic strain amplitude.

III. RESULTS AND DISCUSSION

A. *Monotonic Stress-Strain Curves*

The data acquired during the first quarter cycle of the highest plastic strain amplitude fatigue tests were used as the monotonic stress-strain curves. These results are shown in Figure 2. For both materials, higher stresses were recorded at the fast strain rate compared to the slow strain rate, as expected. There is a smaller difference in stress between the monotonic stress-strain curves for the Nb-1Zr tested at the two rates due to the fact that solute atoms limit edge dislocation mobility, thereby shifting the low-temperature friction stress-controlled regime to higher strain rates (lower temperatures). The absence of a yield point in the CPNb is consistent with the relatively low interstitial content of this material. The curves for Nb-1Zr show an upper yield which we attribute to the pinning of dislocations by the substitutional zirconium atoms.

B. *Elastic Moduli*

In order to calculate the plastic strain, the elastic strain must be subtracted from the total strain. This calculation requires that the elastic modulus be known to a high degree of accuracy. In the present work, the elastic moduli were obtained by deforming specimens well within the elastic limits. The measured moduli were 91.8 and 105.1 GPa for the CPNb and Nb-1Zr metals, respectively. Published modulus values are 105 and 68.9 GPa for CPNb and Nb-1Zr, respectively.[9]

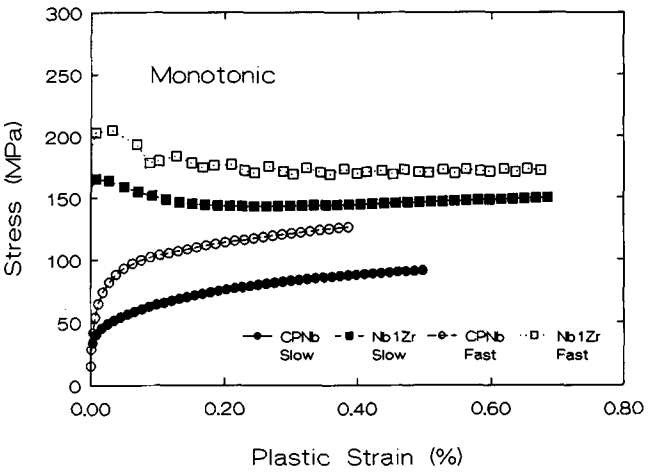

Fig. 2—Monotonic stress-strain curves for commercially pure Nb and Nb-1Zr each at two strain rates.

The difference between the published and measured values for CPNb is probably a result of crystallographic texture in the material used in the present investigation, since the material was not completely recrystallized prior to testing. The reason for the discrepancy in the modulus values for Nb-1Zr is not clear. However, it is difficult to accept that the addition of 1 pct zirconium to niobium would decrease the elastic modulus by one third; for this reason, we believe the published value of 68.9 GPa to be erroneous. The measured value of 105 GPa for Nb-1Zr is certainly more consistent with the accepted modulus value for CPNb.

C. *Cyclic Stress-Strain Response*

For each metal and strain rate, a series of tests was conducted over a range of plastic strain amplitudes. There were no significant differences between the magnitudes of the tension and compression peak stresses, in contrast to single-crystal results, but as expected for polycrystalline material. Figures 3 through 6 illustrate the average (of the tension and compression) peak stress *vs* number of cycles for the two metals tested at the two strain rates. For most specimens, an initial period of rapid hardening was observed, after which the peak stress remained relatively stable. In particular, the results for Nb-1Zr show stable behavior after the initial rapid hardening regime, although a small amount of softening occurred at the high rate (Figure 6). In contrast, the results for CPNb exhibit either stable behavior or a gradual increase in peak stress with increasing number of cycles at the higher plastic strain amplitudes (Figures 3 and 4). In the latter case, the rate of increase in stress is proportional to the plastic strain amplitude.

Cyclic stress-strain (CSS) curves can also be constructed from the present data. The peak stress and plastic strain values from a stable hysteresis loop are obtained

from each test. Plotting and linking these stress-strain data points produces the CSS curve. Most of the tests in this investigation resulted in stable hysteresis loops. For those that did not, the stress and strain values at the middle of the life were used in the construction of the CSS curves. In all cases, the average (of the tension and compression) peak stress was used.

In most cases, an individual specimen was used to obtain each of the CSS data points. An alternative approach for obtaining the CSS is the multiple-step test in which a single specimen is first cycled between set plastic strain limits until a stable hysteresis loop is formed. The plastic strain limit is then increased and the specimen again cycled until another stable hysteresis loop is formed. It has been shown that such tests yield essentially equivalent responses to those of constant amplitude tests provided the material deforms by wavy slip.[10] The CPNb data points for $\Delta\varepsilon_{pl}/2$ from 0.02 to 0.1 pct at the fast strain rate were obtained from a multiple-step test. The validity of the multiple-step data was confirmed, since excellent correlation was obtained with multiple-step and individual specimen data points at plastic strain amplitudes of 0.2, 0.3, and 0.4 pct.

The CSS curves of the two metals, each tested at two strain rates, are shown in Figure 7. Only cyclic hardening was observed, which is typical for annealed metals. The differences in stress for the two rates arises because lattice friction (Peierls stress) limits the mobility

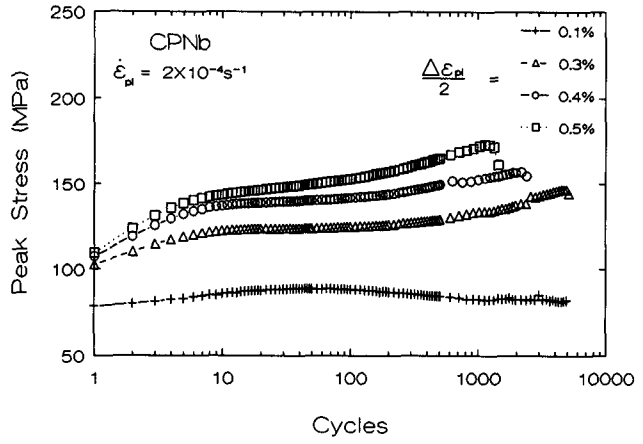

Fig. 3—Peak stress *vs* number of cycles for commercially pure Nb tested at the slow strain rate.

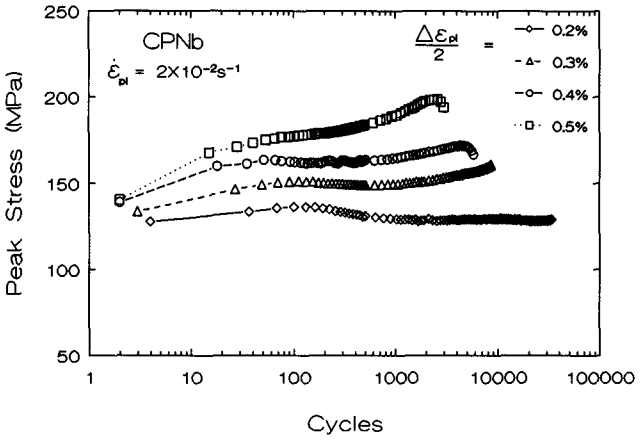

Fig. 4—Peak stress *vs* number of cycles for commercially pure Nb tested at the fast strain rate.

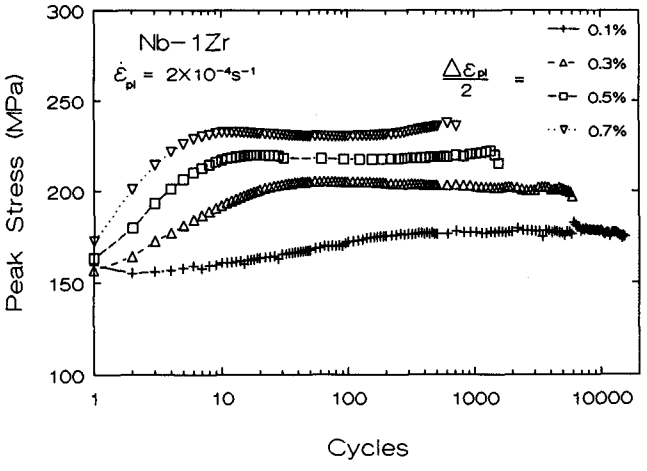

Fig. 5—Peak stress *vs* number of cycles for Nb-1Zr tested at the slow strain rate.

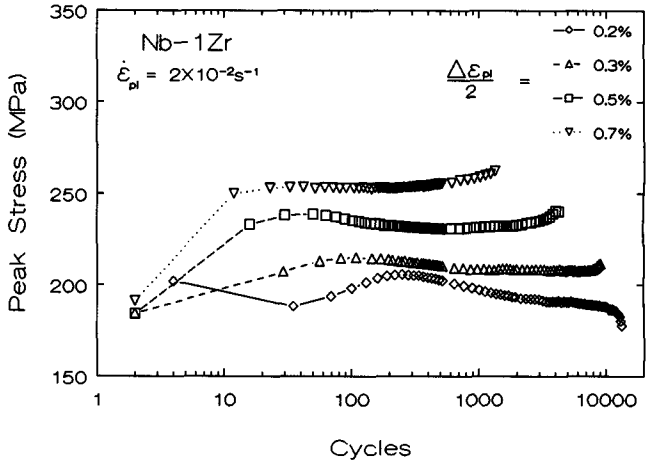

Fig. 6—Peak stress *vs* number of cycles for Nb-1Zr tested at the fast strain rate.

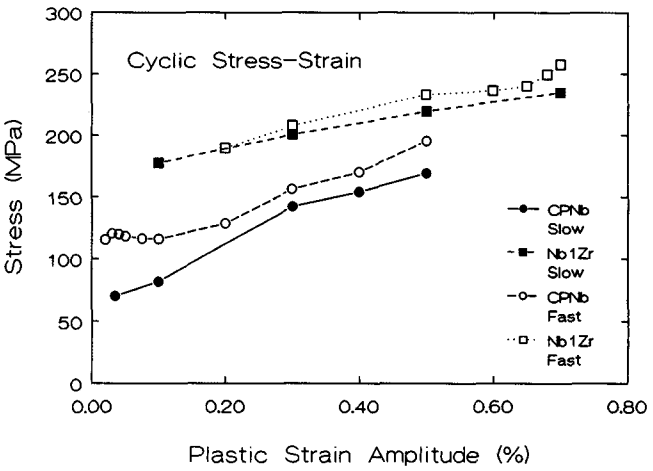

Fig. 7—CSS curves for commercially pure Nb and Nb-1Zr.

of screw dislocations at fast rates (low temperature). As in the case of the monotonic stress-strain curves, there is a smaller difference in stress for the Nb-1Zr tested at the two rates due to the fact that the edge dislocation mobility is limited by the solute atoms.

Another consequence of the limited screw dislocation mobility in bcc metals at fast strain rates is the occurrence of a plateau in the CSS curves at low plastic strain amplitudes. The plateau consists of a range of small plastic strain amplitudes over which the cyclic stress does not vary. Such plateaus have been found in the CSS curves of single crystals of α-iron and α-iron polycrystals[6,11,12] and niobium single crystals.[13,14] It is interesting that for the α-iron polycrystals, the plateau was present under constant plastic strain-rate testing, but not at constant frequency. At the low plastic strain amplitudes of the microplastic plateau and at constant frequency, small variations in plastic strain amplitude cause large variations in the plastic strain rate. For example, at a constant frequency of 10 Hz, changing the plastic strain amplitude from 0.02 to 0.1 pct causes the average plastic strain rate to vary from 8×10^{-3} to 4×10^{-2} s^{-1}. Thus, testing under constant frequency can obscure the microplastic plateau. With α-iron single crystals, this kind of plateau was not observed at slow strain rates.[12] The microplastic plateau is caused by a very low hardening rate due to the restricted mobility of the screw dislocations.[6] This restricted mobility makes dislocation multiplication by irreversible bowing a difficult process. As a consequence, deformation in this regime occurs by the reversible to-and-fro motion of edge dislocations.[13]

As shown in Figure 7, the CPNb material tested at the fast strain rate exhibited a microplastic plateau at plastic strain amplitudes equal to and below 0.1 pct. At the slow strain rate, there was no microplastic plateau. In fact, a microplastic plateau is not expected at the slow strain rate, because the mobilities of the edge and screw dislocations are comparable and, therefore, dislocation multiplication should not be restricted. In a similar manner, the Zr atoms lower the mobility of edge dislocations in the Nb-1Zr alloy to a level comparable to that of screw segments, and a microplastic plateau is not expected at either strain rate. For this reason, as well as the operational difficulty of testing this material at plastic strain amplitudes in the region of the upper yield point, the low strain behavior of Nb-1Zr was not explored in this work.

The data of Mughrabi and co-workers[13,14] exhibit a microplastic plateau in niobium single crystals at plastic strain amplitudes less than 0.05 pct with a plateau stress of 20 MPa. Mughrabi used a Schmid factor of 0.5; hence, the plateau shear stress was 10 MPa. Assuming a Taylor factor of 3, the equivalent polycrystalline tensile stress is 30 MPa. The results of this investigation, presented in Figure 7, show a microplastic plateau at plastic strain amplitudes less than 0.1 pct with a plateau tensile stress of 115 MPa. The large difference in plateau stress is attributed to the very high purity of the crystals used by Mughrabi and to the fact that single crystals are generally much softer due to the lack of grain size strengthening.

The existence of the microplastic plateau has been proposed as the physical basis for the fatigue limit in iron.[13] In conventional fatigue tests, the strain rate is high, indicating that the mobility of screw dislocations should be restricted. When the plastic strain range is small, the plastic strain can be accommodated by the reversible motion of the edge dislocations without microstructural changes and without noticeable cyclic hardening. Therefore, at high strain rates, Mughrabi[6] has suggested that the fatigue limit of bcc metals should ". . . correspond rather well to the plateau of the cyclic stress-strain curve and should lie slightly below the macroscopic yield stress of the virgin material measured at the strain-rate of the fatigue tests." The 0.2 pct offset yield strength measured at the fast strain rate was 124 MPa, which is only slightly higher than the microplastic plateau stress of 110 MPa, in agreement with this prediction. A fatigue limit for polycrystalline niobium[9] is listed as 138 MPa, which is roughly comparable to the 110 MPa plateau stress measured in the present study. Thus, the results of this investigation support the concept that the limited mobility of screw dislocations in the microplastic plateau is the physical basis for the fatigue limit.

The absence of a microplastic plateau at the slow strain rate suggests the lack of a fatigue limit. This observation has important engineering implications, since our practical understanding of fatigue in bcc metals (including steel) is based on the concept of a fatigue limit. However, most fatigue tests are conducted at high rates to minimize testing time, whereas service conditions may impose lower loading rates where the intrinsic material behavior is different. It may be necessary to reconsider the concept of the fatigue limit in light of the fundamental effects of strain rate and solute content on dislocation mobility.

D. *Intergranular Crack Initiation*

As noted earlier, the low-temperature (high strain rate) deformation of bcc metals is dominated by the mechanisms of screw dislocation glide. One important aspect of this behavior is the slip plane and stress asymmetry between tension and compression loading of single crystals, which leads to a large change in shape after many cycles. In polycrystalline bcc metals, however, a macroscopic tension/compression asymmetry is not expected. Instead, the effect of the individual grain shape changes due to local tension/compression asymmetry under cyclic loading at high strain rates is to make intergranular cracking more probable. In experiments on iron-based alloys, Magnin and Driver[15] found that fatigue crack initiation was intergranular at high strain rates and transgranular at low strain rates. This observation is consistent with the expected glide behavior of screw dislocations at the two rates. Even without the tension/compression asymmetry in individual crystals, some incompatible deformation occurs, but the tension/compression asymmetry accentuates the incompatible deformation, thus increasing the probability of intergranular cracking. The CPNb and Nb-1Zr specimens tested at the fast strain rate exhibited intergranular secondary cracking, as shown in Figure 8. In contrast, there were no cracks that could be clearly identified as intergranular cracks in the CPNb or Nb-1Zr specimens tested at the slow strain rate.

E. *Cyclic Life*

Figure 9 illustrates the fatigue-life data (Coffin-Manson plot) of plastic strain amplitude *vs* number of reversals

to failure. We note that this plot does not include data at strain amplitudes in the microplastic plateau, since the specimens were not tested to failure in this regime. As mentioned previously, both 90- and 180-deg extensometer knife edges were used in the present experiments. The data form two nearly parallel lines. In the lower line, all of the specimens, except one, were tested with the 90-deg knife edges. In the upper line, all specimens were tested with 180-deg knife edges. The upper and lower lines drawn in Figure 9 are linear fits to the logarithmic data for the 180-deg (blunt) and 90-deg (sharp) knife edges, respectively. The deeper impressing 90-deg knife edges caused shorter life relative to the 180-deg knife edges; this was confirmed in duplicate tests of Nb-1Zr at a plastic strain amplitude of 0.5 pct. Thus, the offset between the two lines formed by the data can be attributed entirely to the use of different knife edges. We conclude that there is no significant difference in cyclic life between the two metals and there is no influence of strain rate on cyclic lifetime. However, a strain-rate effect on lifetime would be expected of specimens tested to failure in the microplastic plateau regime.

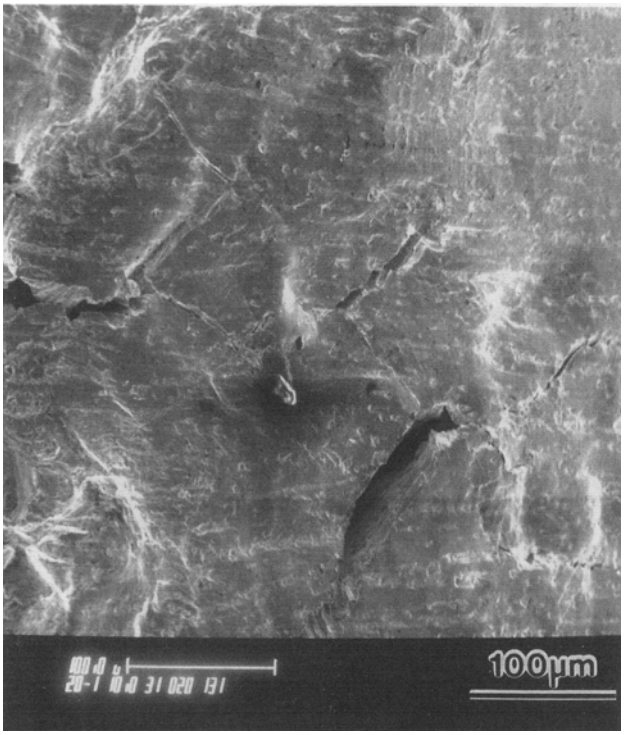

Fig. 8—Intergranular cracking observed in a commercially pure Nb specimen tested at the fast strain rate and a plastic strain amplitude of 0.2 pct.

F. *Hysteresis Loop Analysis*

During the course of this investigation, it was noted that although the peak stress did not vary significantly with increasing numbers of cycles, the shape of the hysteresis loops did change. As a consequence, a detailed analysis of the hysteresis loops produced during low-cycle fatigue testing was conducted in order to determine the friction stress and back stress components for each loop, following a procedure outlined by Kuhlmann-Wilsdorf and Laird.[16] For each loop, a peak stress, σ_p, and a yield stress, σ_y, can be identified with both right and left sides of the loop, as shown in Figure 10. The friction stress, σ_f, and back stress, σ_b, are simply determined as follows:

$$\sigma_p = \sigma_f + \sigma_b \quad [3]$$

$$\sigma_y = \sigma_f - \sigma_b \quad [4]$$

Rearranging,

$$\sigma_f = \left(\frac{\sigma_p + \sigma_y}{2}\right) \quad [5]$$

$$\sigma_b = \left(\frac{\sigma_p - \sigma_y}{2}\right) \quad [6]$$

The value of the yield stress, however, is somewhat arbitrarily determined, just as the monotonic yield strength is dependent on the arbitrary choice of an offset (typically 0.2 pct) as the defining value. In the present analysis, the data points between 0.4 and 0.8 times the peak stress were used to define a straight line (determined from a least-squares fit), since this was the most linear section of that part of the loop. Another straight line parallel to

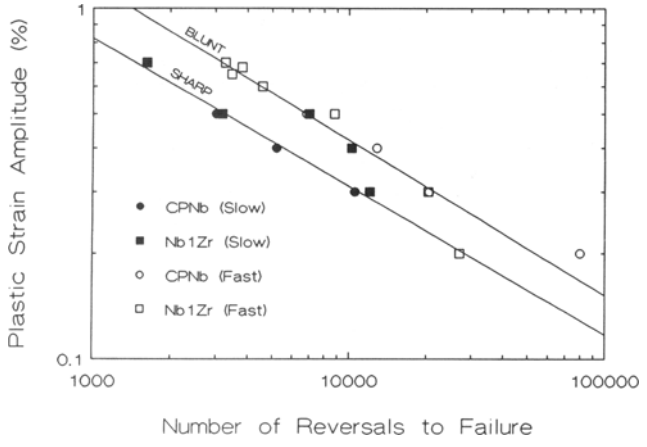

Fig. 9—Coffin-Manson plot for commercially pure Nb and Nb-1Zr.

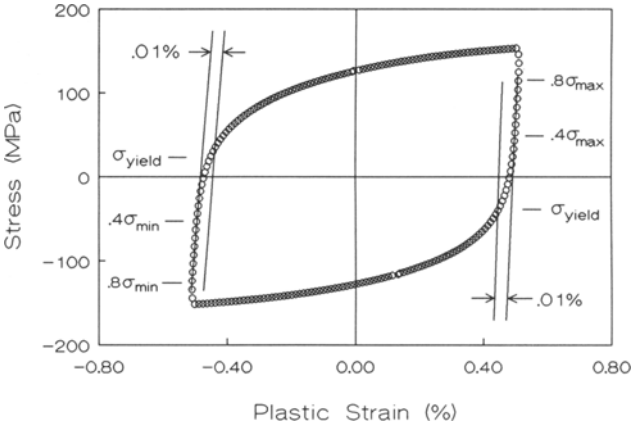

Fig. 10—Hysteresis loop showing definition of yield stress.

the first, but offset from it by 0.01 pct strain, was constructed. The yield stress was defined as the intersection of this second line with the hysteresis loop. A constant offset parameter of 0.01 pct strain was used for all tests; therefore, at least the relative values of the friction and back stresses are meaningful.

The peak stresses of the Nb-1Zr samples at both slow and fast strain rates were constant after the short rapid hardening of the first few cycles. Constant peak stresses are often considered to indicate a stable mechanical and microstructural condition. However, the hysteresis loop analysis demonstrates that the constant peak stresses for Nb-1Zr were a result of the increasing back stress compensating for the decreasing friction stress component. An example of this result is shown in Figure 11. Thus, a constant peak stress does not necessarily mean a stable condition during cyclic deformation.

The following comments also pertain to the behavior after the initial rapid hardening phase of the first few cycles. As shown in Figures 4 and 5, the plots of peak stress *vs* number of cycle for the CPNb samples tested

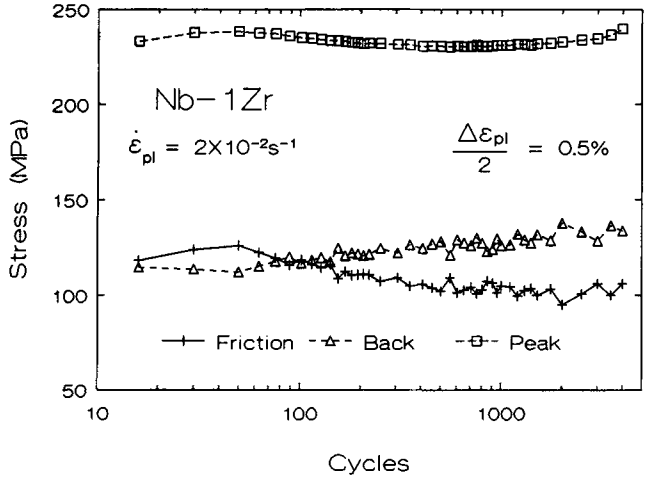

Fig. 11—Variation of friction stress, back stress, and peak stress with cycles in Nb-1Zr.

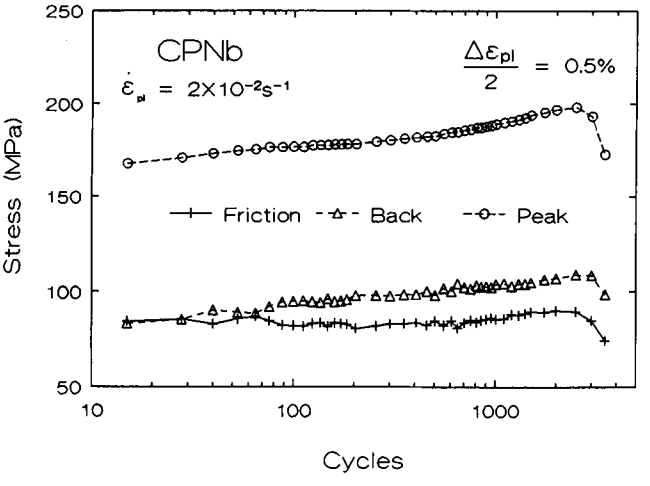

Fig. 12—Variation of friction stress, back stress, and peak stress with cycles in commercially pure Nb.

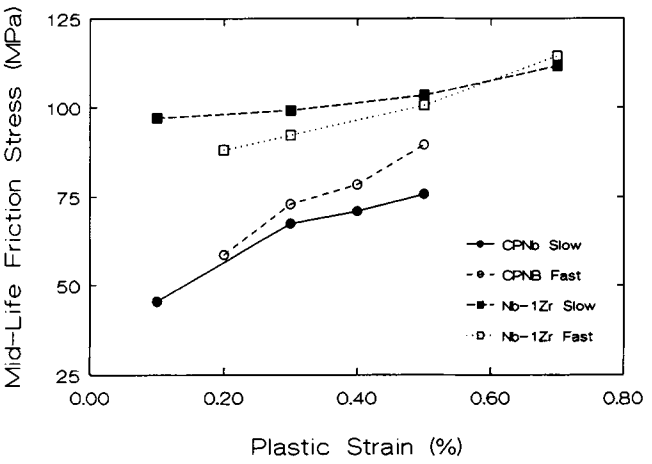

Fig. 13—Variation of friction stress with plastic strain amplitude.

at plastic strain amplitudes of 0.3, 0.4, and 0.5 pct showed slight but gradually increasing peak stress with increasing numbers of cycles. The results of the hysteresis loop analysis demonstrate that the increasing peak stress was due to an increasing back stress; the friction stress remained essentially constant, as indicated in the example shown in Figure 12. A comparison of Figures 11 and 12 shows a similarity of increasing back stress with increasing numbers of cycles for both metals. In contrast, the friction stress remained constant during cycling of CPNb and gradually decreased in Nb-1Zr.

The two metals also exhibited a different effect of strain rate on the friction stress. It can be seen in Figure 13 that the results for CPNb always exhibit a greater friction stress at the fast strain rate compared to the slow strain rate. This was not true for Nb-1Zr, where three out of four samples exhibited a lower friction stress at the fast strain rate. In CPNb, the friction stress has a strong Peierls stress component, which accounts for its strain-rate sensitivity. In Nb-1Zr, the friction stress is dominated by the zirconium atoms, and the Peierls stress component is negligible at room temperature, with the consequence that the strain-rate sensitivity of the friction stress is greatly reduced.

IV. CONCLUSIONS

Commercially pure niobium and niobium-1 pct zirconium were tested under low-cycle fatigue conditions at ambient temperature. Each metal was tested at slow (2×10^{-4} s^{-1}) and fast (2×10^{-2} s^{-1}) strain rates.

1. Only cyclic hardening occurred in both metals at each strain rate.
2. The cyclic stresses were always higher in the fast strain-rate tests than in the slow strain-rate tests at the same plastic strain amplitude. The difference between the fast and slow strain-rate cyclic response is greater for commercially pure niobium than for niobium-1 pct zirconium. The different responses of the two metals are attributed to the fact that the edge and screw dislocation mobilities are more nearly equal in niobium-1 pct zirconium as a result of the interaction between

the edge dislocations and the zirconium substitutional atoms.

3. The expected behavior for these bcc metals in the low-temperature (fast strain-rate) regime, where screw dislocation mobility is limited, was observed. Specifically, intergranular cracking occurred, and a microplastic plateau was observed in the commercially pure material. A microplastic plateau was not detected at the lower strain rate.
4. The presence of the microplastic plateau and the cyclic stress amplitude of this plateau support the proposal that the limited mobility of screw dislocations in the microplastic plateau is the physical origin of the fatigue limit.
5. At plastic strains above the microplastic plateau, both metals have the same fatigue life at equal plastic strain amplitudes. The strain rate had no effect on the cyclic lifetime.
6. The mechanisms of cyclic deformation in polycrystalline niobium are consistent with previously published descriptions of single-crystal behavior.
7. An analysis of the hysteresis loops demonstrates that a constant peak stress does not necessarily indicate a constant substructure, as reflected in variations of the friction and back stress components.

ACKNOWLEDGMENTS

Funding for the work described in this article was provided by the Air Force Office of Scientific Research under Grant No. 89-0287. We gratefully acknowledge the support and encouragement of the program manager, Dr. Alan H. Rosenstein.

REFERENCES

1. F. Ackermann, H. Mughrabi, and A. Seeger: *Acta Metall.*, 1983, vol. 31, pp. 1353-66.
2. M. Anglada and F. Guiu: *Phil. Mag. A*, 1981, vol. 44, pp. 499-522.
3. M. Anglada and F. Guiu: *Phil. Mag. A*, 1981, vol. 44, pp. 523-41.
4. C. English: in *Niobium-Proc. Int. Symp.*, H. Stuart, ed., TMS-AIME, Warrendale, PA, 1984, pp. 239-324.
5. D.W. Chung and N.S. Stoloff: *Metall. Trans. A*, 1978, vol. 9A, pp. 1387-99.
6. H. Mughrabi, K. Herz, and X. Stark: *Int. J. Fract.*, 1981, vol. 17, pp. 193-220.
7. L.N. Chang, G. Taylor, and J.W. Christian: *Acta Metall.*, 1983, vol. 31, pp. 37-42.
8. D. Hull and D.J. Bacon: *Introduction to Dislocations*, 3rd ed., Pergamon Press, Oxford, United Kingdom, 1984, p. 124.
9. *Metals Handbook*, 9th ed., ASM, Metals Park, OH, 1980, vol. 3, p. 333.
10. J.W. Martin and L. Edwards: in *Micromechanisms of Plasticity and Fracture*, Parsons Press, Trinity College, Dublin, 1983, pp. 333-68.
11. H. Mughrabi: *Scripta Metall.*, 1979, vol. 13, pp. 479-84.
12. H. Mughrabi, K. Herz, and F. Ackermann: *Proc. 4th Int. Conf. on the Strength of Metals and Alloys*, Laboratoire de physique du solide, Nancy, France, 1976, pp. 1244-48.
13. H. Mughrabi: in *Dislocations and Properties of Real Materials*, Institute of Metals, London, 1985, pp. 244-62.
14. H. Mughrabi: *Proc. 5th Int. Conf. on the Strength of Metals and Alloys*, P. Haasen, V. Gerold, and G. Kosterz, eds., Pergamon Press, Oxford, United Kingdom, 1980, pp. 1615-38.
15. T. Magnin and J.H. Driver: in *Low Cycle Fatigue and Life Prediction*, ASTM STP 770, C. Amzallag, B.N. Leis, and P. Rabbe, eds., ASTM, Philadelphia, PA, 1982, pp. 212-26.
16. D. Kuhlmann-Wilsdorf and C. Laird: *Mater. Sci. Eng.*, 1979, vol. 37, pp. 111-20.